

Edge states and determination of pairing symmetry in superconducting Sr_2RuO_4

K. Sengupta, Hyok-Jon Kwon, and Victor M. Yakovenko

Department of Physics and Center for Superconductivity Research, University of Maryland, College Park, MD 20742-4111
(cond-mat/0106198, v.1: June 11, 2001; v.2: September 2, 2001)

We calculate the energy dispersion of the surface Andreev states and their contribution to tunneling conductance for the order parameters with horizontal and vertical lines of nodes proposed for superconducting Sr_2RuO_4 . For vertical lines, we find double peaks in tunneling spectra reflecting the van Hove singularities in the density of surface states originating from the turning points in their energy dispersion. Comparison with the experimental data on tunneling in Sr_2RuO_4 supports the p - or f -wave with horizontal lines of nodes, for which we find a cusp-like peak at zero bias.

PACS numbers: 74.70.Pq, 74.80.Fp, 73.20.-r

Numerous experiments suggest that the superconducting state of Sr_2RuO_4 [1] is unconventional (see review [2]). Strong suppression of T_c by non-magnetic impurities [3] and absence of the Hebel-Slichter peak in NMR experiments [4] indicate that it is not s -wave. The absence of spin susceptibility reduction below T_c in the Knight shift measurements indicates the spin-triplet pairing [5]. The μSR experiment suggests a superconducting state with broken time-reversal symmetry [6]. Small-angle neutron scattering reveals a square vortex lattice, which is interpreted as the indication for a two-component order parameter [7]. These experiments initially led to suggestion of the 2D chiral (time-reversal non-invariant), isotropic, nodeless p -wave pairing potential [8]. However, the power-law temperature dependences found in specific heat [9], nuclear relaxation rate [10], penetration depth [11], thermal conductivity [12], and ultrasonic attenuation [13,14] indicate nodes in the energy gap. In response to these experiments, the following alternative order parameters were proposed [15]: anisotropic p -wave [16], p -wave with the so-called horizontal lines of nodes [17], and f -waves with vertical [17,18] or horizontal lines of nodes [19]. It was also proposed that the α and β bands of Sr_2RuO_4 are either not superconducting [20] or have horizontal lines of nodes [21]. Big in-plane anisotropy of ultrasound attenuation [14] supports the vertical lines of nodes. However, thermal conductivity depends very little on the orientation of an in-plane magnetic field [22], which is against the vertical lines [23].

Electron tunneling between a normal metal and a superconductor proved to be an important tool in determining superconducting symmetry. Observation of the zero-bias conductance peak (ZBCP) [24] due to formation of the midgap Andreev bound states [25] confirmed the d -wave symmetry of the high- T_c cuprates. Electron tunneling in Sr_2RuO_4 was studied theoretically in Refs. [26] and [27] for the 2D isotropic chiral unitary and non-unitary p -waves. In this paper, we calculate the tunneling conductance curves for the alternative order parameters listed above and compare them with experiments [28,29].

We model the tunneling contact by two semi-infinite

regions, normal (N) and superconducting (S), with a flat interface (I) perpendicular to the a axis of Sr_2RuO_4 (see Fig. 1). The x and y axes are selected along the crystal axes a and b , respectively. The tunneling conductance is calculated at zero temperature by solving the Bogoliubov-de Gennes equations in the ballistic regime following Refs. [30,31]. The tunneling barrier is modeled by a delta-function potential of strength \mathcal{H} , so the boundary conditions at the interface are $\psi_n|_I = \psi_s|_I$ and $\hat{v}_n\psi_n|_I = \hat{v}_s\psi_s|_I - 2i\mathcal{H}\psi_n|_I$. Here ψ_n and ψ_s are the electron wave functions in the normal and superconducting regions, and $\hat{v}_{n,s}$ are the velocity components perpendicular to the interface. The pairing potential of a triplet superconductor can be expressed as $\hat{\Delta} = i\sigma_y(\boldsymbol{\sigma} \cdot \mathbf{d})\Delta(\mathbf{k}, x)$, where $\boldsymbol{\sigma}$ are the Pauli matrices operating on the electron spin indices, the vector \mathbf{d} indicates the direction of spin polarization, and \mathbf{k} is the relative momentum of electrons in a Cooper pair. In this paper, we consider the cases where \mathbf{d} does not depend on \mathbf{k} and is pinned to the c axis of Sr_2RuO_4 . The spatial dependence of the pairing potential is taken to be step-like: $\Delta(\mathbf{k}, x) = \Delta(\mathbf{k})\Theta(x)$. Assuming that the electron momentum k_y parallel to the interface is conserved, the tunneling conductance per one layer, $\overline{G}(V)$, can be written as an integral over k_y [30,31]:

$$\overline{G}(V) = \frac{2e^2}{h} l \int_{-k_y^{\max}}^{k_y^{\max}} \frac{dk_y}{h} G(V, k_y), \quad (1)$$

$$G(V, k_y) = D \frac{1 + |\Gamma|^2 D - (1 - D) |\Gamma|^4}{|1 - (1 - D) \Gamma^2 \exp(i\Phi)|^2}. \quad (2)$$

In Eq. (1), e is the electron charge, h is the Planck constant, l is the length of the interface, and V is the bias voltage. We consider the case where the Fermi surfaces of both the normal metal and superconductor are circular, and their radii are $k_F^{(n)} > k_F^{(s)}$, as shown in Fig. 1. The limits of integration are set by the smaller Fermi momentum: $k_y^{\max} = k_F^{(s)}$. In Eq. (2), $D(k_y) = 4v_n(k_y)v_s(k_y)/\{[v_n(k_y) + v_s(k_y)]^2 + 4\mathcal{H}^2\}$ is the normal-state transmission coefficient, where $v_{n,s}(k_y)$ are the Fermi velocities components perpendicular to the interface. $\Phi(k_y) = \phi_A(k_y) - \phi_B(k_y)$ is the phase difference

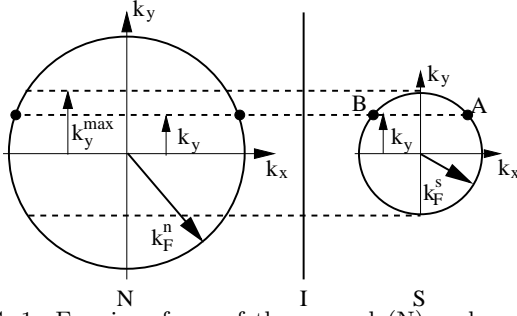


FIG. 1. Fermi surfaces of the normal (N) and superconducting (S) materials forming the interface I. The points A and B on the Fermi surface S are connected by specular reflection from the interface.

of the superconducting pairing potentials at the points on the Fermi surface connected by electron reflection from the interface (points A and B in Fig. 1) [31]. $\Gamma(V, k_y)$ is

$$\Gamma = \frac{eV - \text{sgn}(eV)\sqrt{(eV)^2 - |\Delta(k_y)|^2}}{|\Delta(k_y)|}, \quad |eV| \geq |\Delta|,$$

$$\Gamma = \frac{eV - i\sqrt{|\Delta(k_y)|^2 - (eV)^2}}{|\Delta(k_y)|}, \quad |eV| \leq |\Delta|. \quad (3)$$

Denoting $G(V, k_y)$ as $\mathcal{G}(V, k_y)$ for the subgap voltage $|eV| \leq |\Delta|$, where $|\Gamma(V)| = 1$, we rewrite Eq. (2) as

$$\mathcal{G}(V, k_y) = \frac{D^2(k_y)/2[1 - D(k_y)]}{D^2(k_y)/4[1 - D(k_y)] + F^2(V, k_y)}, \quad (4)$$

$$F = \sqrt{1 - |eV/\Delta|^2} \cos(\Phi/2) - (eV/|\Delta|) \sin(\Phi/2). \quad (5)$$

For a high barrier, $D \approx v_n v_s / \mathcal{H}^2 \ll 1$. Then Eq. (4) becomes $\mathcal{G}(V, k_y) \approx \pi D(k_y) \delta[F(V, k_y)]$, and Eq. (1) gives

$$\bar{\mathcal{G}}(V) \approx C \int_{-k_y^{\max}}^{k_y^{\max}} dk_y v_n(k_y) v_s(k_y) \delta[F(V, k_y)], \quad (6)$$

where $C = 2\pi e^2 l / h^2 \mathcal{H}^2$. The delta-function contributes to the integral (6) when $F(V, k_y) = 0$. Using Eq. (5), this condition can be written as $eV = E(k_y)$, where

$$E(k_y) = |\Delta(k_y)| \cos[\Phi(k_y)/2] \quad (7)$$

for $\sin(\Phi/2) \geq 0$, i.e. $0 \leq \Phi \leq 2\pi$, which is the appropriate interval for Φ . $E(k_y)$ is nothing but the energy of a surface state with the momentum k_y obtained for the impenetrable barrier ($\mathcal{H} \rightarrow \infty$) [25]. The energy density of these surface states (DOS) is

$$\rho(\epsilon) = \int_{-k_F^{(s)}}^{k_F^{(s)}} \frac{dk_y}{h} \delta[\epsilon - E(k_y)] = \sum_j \frac{1}{h |\partial_{k_y^{(j)}} E(k_y^{(j)})|}, \quad (8)$$

where $k_y^{(j)}$ is the j -th root of the equation $E(k_y) = \epsilon$.

The delta-function in Eq. (6) indicates that the subgap tunneling takes place when the bias voltage matches the

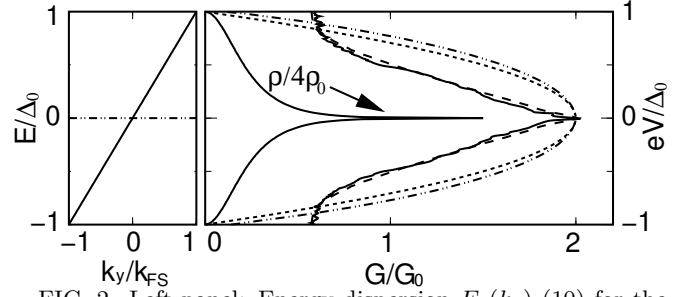


FIG. 2. Left panel: Energy dispersion $E_1(k_y)$ (10) for the 2D isotropic p -wave. Right panel: The corresponding exact [Eqs. (1) and (2), dash-dotted line] and approximate [Eq. (11), dotted line] tunneling conductance curves; DOS (solid line with the arrow) and tunneling conductance (long-dashed line) for the p -wave with horizontal lines of nodes [Eq. (18)]. Solid line: Experimental curve from Fig. 2 of Ref. [29] for 0.8 K.

energy of a surface state: $eV = E(k_y)$. Denoting the j -th root of this equation as $k_y^{(j)}$ and resolving the delta-function in Eq. (6), we find

$$\bar{\mathcal{G}}(V) \approx C \sum_j \frac{v_n(k_y^{(j)}) v_s(k_y^{(j)}) \sqrt{|\Delta(k_y^{(j)})|^2 - (eV)^2}}{|\partial_{k_y^{(j)}} E(k_y^{(j)})|}. \quad (9)$$

Because the denominators in Eqs. (9) and (8) are the same, both expressions exhibit peaks (the inverse-square-root van Hove singularities) at the turning points of the energy dispersion, where $\partial_{k_y} E(k_y) = 0$. Their positions depend solely on the pairing potential $\Delta(k_y)$ through Eq. (7) and not on the band structure details. The number of such turning points does not change upon small continuous deformation of $\Delta(k_y)$, so it is a topological feature. Because of the additional factors in Eq. (9), tunneling conductance is not simply proportional to DOS, as often assumed. Eq. (9) vanishes at $k_y \rightarrow k_F^{(s)}$, where the normal component v_s of the Fermi velocity goes to zero. It also vanishes when $\Delta(k_y) \rightarrow 0$ or $E(k_y) \rightarrow \pm\Delta(k_y)$ (i.e. $\Phi(k_y) \rightarrow 0, 2\pi$). In these cases, the quasiparticle localization length perpendicular to the interface, $\lambda = \hbar v_s / \sqrt{|\Delta|^2 - E^2}$, diverges [25]; thus, the probability to find a quasiparticle on the surface vanishes.

In Figs. 2, 3, 4, and 5, we show how these general equations apply to the alternative superconducting order parameters proposed for Sr_2RuO_4 in the literature. In order to focus on the features of superconductor, rather than normal metal, we took $k_F^{(n)} = 5k_F^{(s)}$. Then, the perpendicular velocity of the normal metal is approximately constant for all momenta $|k_y| \leq k_F^{(s)}$: $v_n \approx v_F^{(n)}$, while in the superconductor it is $v_s = v_F^{(s)} \sqrt{1 - (k_y/k_F^{(s)})^2}$, where $v_F^{(n)}$ and $v_F^{(s)}$ are the corresponding Fermi velocities. The calculations are done for the high barrier $Z = \mathcal{H} / \sqrt{v_F^{(n)} v_F^{(s)}} = 3$. As the figures illustrate, in this limit, the approximate curves given by Eq. (9), which includes only the localized surface states, agree well with

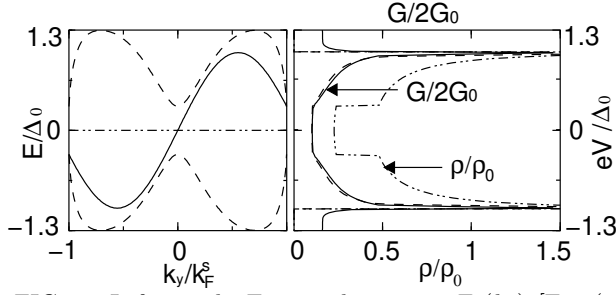


FIG. 3. Left panel: Energy dispersion $E_2(k_y)$ [Eq. (13), solid line] and gap $|\Delta_2(k_y)|$ [Eq. (12), dashed line] for the anisotropic p -wave. Right panel: the corresponding DOS [dashed-dotted line] and the exact (solid line) and approximate [dashed line] tunneling conductance curves.

the exact curves obtained from Eqs. (1) and (2), which also include the contribution of the extended bulk states.

For the 2D isotropic chiral p -wave, the pairing potential and the energy dispersion of the edge states are [8,27]

$$\Delta_1(\mathbf{k}) = \Delta_0(k_x + ik_y)/k_F^{(s)}, \quad E_1(k_y) = \Delta_0 k_y/k_F^{(s)}. \quad (10)$$

Substituting Eq. (10) into Eqs. (9) and (8), we find

$$\bar{G}(V) \approx 2G_0 \left[1 - \left(\frac{eV}{\Delta_0} \right)^2 \right], \quad \rho(\epsilon) = \frac{k_F^{(s)}}{h\Delta_0} = \rho_0. \quad (11)$$

where $G_0 = \pi e^2 l k_F^{(s)} v_F^{(n)} v_F^{(s)} / h^2 \mathcal{H}^2$ is the normal-state conductance, achieved at $|eV| \gg |\Delta|$. The energy dispersion (10) has no turning points, thus DOS is flat, and the tunneling conductance curve is parabolic (Fig. 2) [26,27].

For the anisotropic chiral p -wave proposed in Ref. [16], the pairing potential and the energy dispersion are

$$\Delta_2(\mathbf{k}) = \Delta_0 [\sin(k_x a / \hbar) + i \sin(k_y a / \hbar)], \quad (12)$$

$$E_2(k_y) = \Delta_0 \sin(k_y a / \hbar), \quad (13)$$

where a is the lattice constant, and $k_F^{(s)} a = 0.9\pi\hbar$. Substituting Eqs. (12) and (13) into Eqs. (1), (2), (3), (9) and (8), we calculate the tunneling conductance and DOS curves shown in Fig. 3. They exhibit peaks at $eV = \pm\Delta_0$ originating from the turning points in the edge states dispersion. Equation $eV = E(k_y)$ has one solution $k_y^{(j)}$ for $|eV| < 0.31\Delta_0$ and two solutions for $0.31\Delta_0 < |eV| < \Delta_0$. The switch causes the discontinuity of DOS and the slope change of tunneling conductance at $eV = \pm 0.31\Delta_0$.

For the f -wave proposed in Ref. [17], we have

$$\Delta_3(\mathbf{k}) = \Delta_0 (k_x^2 - k_y^2) (k_x + ik_y) / (k_F^{(s)})^3, \quad (14)$$

$$E_3(k_y) = \Delta_0 |k_x^2 - k_y^2| k_y / (k_F^{(s)})^3. \quad (15)$$

As shown in Fig. 4, the edge states dispersion has cusps at $k_y = \pm k_F^{(s)} / \sqrt{2}$, where $\Delta_3(\mathbf{k})$ vanishes, and two turning

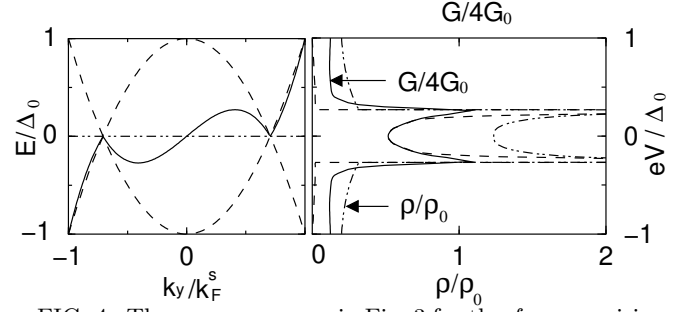


FIG. 4. The same curves as in Fig. 3 for the f -wave pairing potential (14) with vertical lines of nodes.

points in between. Consequently, the tunneling conductance and DOS curves have peaks at $eV = \pm 0.26\Delta_0$.

For another f -wave proposed in Refs. [17,18], we have

$$\Delta_4(\mathbf{k}) = 2\Delta_0 k_x k_y (k_x + ik_y) / (k_F^{(s)})^3, \quad (16)$$

$$E_4(k_y) = 2\Delta_0 k_x^2 k_y / (k_F^{(s)})^3. \quad (17)$$

Eqs. (16) and (17) transform into Eqs. (14) and (15) upon a $\pi/4$ rotation in the x - y plane. As shown in Fig. 5, the turning points in the energy dispersion and the peaks in the tunneling conductance and DOS curves occur at $eV = \pm 0.76\Delta_0$. Their position is approximately the same as in Fig. 3 for the anisotropic p -wave. However, in Fig. 5, unlike in all other figures, tunneling conductance vanishes at zero bias, even though DOS remains finite. This characteristic feature of the f -wave potential (16) is a consequence of the square-root factor in Eq. (9).

Thus far we considered the order parameters that do not depend on k_z , the momentum perpendicular to the Sr_2RuO_4 planes. Ref. [17] also proposed the p -wave with horizontal lines of nodes at certain k_z , which can be obtained from Eq. (10) by the following substitution

$$\Delta_0 \rightarrow \tilde{\Delta}_0(k_z) = \Delta_0 \cos(k_z c / \hbar), \quad (18)$$

where c is the interplane distance. Now DOS is obtained by averaging $\rho(\epsilon)$ from Eq. (11) over k_z using Eq. (18). At the nodes, $\tilde{\Delta}_0(k_z)$ vanishes linearly with k_z , thus the averaging results in a logarithmic singularity in $\rho(\epsilon)$ at $\epsilon \rightarrow 0$, as shown in Fig. 2. When averaging $\bar{G}(V)$ over k_z , the divergence of $1/\tilde{\Delta}_0^2(k_z)$ at the node must be cut off at $|eV|$, because Eq. (11) applies only for $|eV| < |\tilde{\Delta}_0(k_z)|$. Thus, we find $\bar{G}(V) \approx 2G_0 [1 - (4/\pi) |eV|/\Delta_0]$ for $|eV| \ll \Delta_0$. This equation and the numerically calculated curve shown in Fig. 2 demonstrate that tunneling conductance has a cusp at zero bias. This cusp and the logarithmic singularity of DOS result from the pile-up of surface states at zero energy caused by vanishing gap. So they are robust features of the pairing potentials with horizontal lines of nodes independent of the band structure details. The f -wave with horizontal lines of nodes [19],

$$\Delta_6(\mathbf{k}) = i\Delta_0 \sin(k_z c / \hbar) (k_x + ik_y)^2 / (k_F^{(s)})^2, \quad (19)$$

$$E_6(k_y) = \text{sgn}(k_y) \Delta_0 [2(k_y/k_F^{(s)})^2 - 1] |\sin(k_z c / \hbar)|, \quad (20)$$

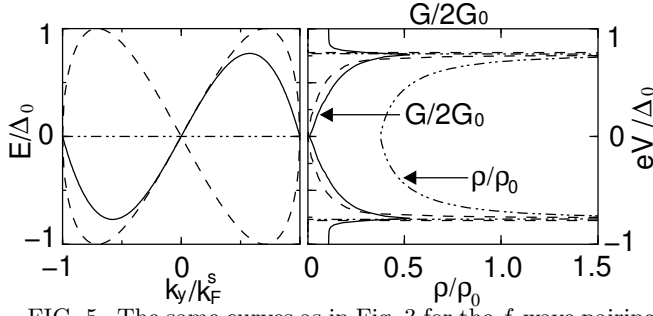


FIG. 5. The same curves as in Fig. 3 for the f -wave pairing potential (16) with vertical lines of nodes.

produces similar curves for the in-plane tunneling. However, being an odd function of k_z , it also exhibits a ZBCP in the c -axis tunneling.

Point-contact tunneling spectroscopy [28] found a ZBCP in Sr_2RuO_4 . The data were fitted using the 2D isotropic p -wave (10) and assuming a narrow acceptance cone, i.e. a small value of k_y^{max} . In this situation, only the states with $k_y \approx 0$ and hence $E(k_y) \approx 0$ are probed; thus all pairing potentials, except the f -wave (16), would show a ZBCP. However, such a ZBCP, in contrast to nonchiral cuprates [25] and organic superconductors [32], does not identify the pairing symmetry uniquely.

The more recent tunneling experiment [29], performed on Sr_2RuO_4 with inclusions of Ru, found a cusp-like peak at zero bias in the 1.4-K phase and a sharper ZBCP in the 3-K phase. The latter was attributed to a nonchiral superconductivity developing at the grain boundaries [33]. An experimental curve from Ref. [29] representing the 1.4-K phase is shown in Fig. 2. It agrees well with our curve calculated for the pairing potential (18). Such a good fit is a strong indication in favor of the p - or f -wave pairing potential with horizontal lines of nodes in the 1.4-K phase. Further measurements showing the absence or presence of a ZBCP in the c -axis tunneling could discriminate between the p - and f -wave cases. Experiment [29] found that an additional sharp ZBCP develops on top of the cusp at lower temperatures 0.5 and 0.32 K. It may be attributed to a contribution from the c -axis tunneling, if the pairing potential is the f -wave (19).

In conclusion, we derived an analytical formula for sub-gap tunneling at low barrier transparency, which takes into account only the contribution of the surface Andreev states. This formula produces tunneling curves in a simple and physically transparent way. For the pairing potentials with vertical lines of nodes, tunneling curves show double peaks originating from the turning points in the energy dispersion of the surface Andreev states. Such double peaks have not been observed experimentally in Sr_2RuO_4 . On the other hand, for the p - and f -waves with horizontal lines of nodes, we found a single cusp at zero bias that well fits the experimental data [29].

[1] Y. Maeno *et al.*, Nature (London) **372**, 532 (1994).

[2] Y. Maeno, T. M. Rice, and M. Sigrist, Physics Today **54**, #1, 42 (January 2001); **54**, #3, 104 (March 2001).
[3] A. P. Mackenzie *et al.*, Phys. Rev. Lett. **80**, 161 (1998); Z. Q. Mao, Y. Mori, and Y. Maeno, Phys. Rev. B **60**, 610 (1999).
[4] K. Ishida *et al.*, Phys. Rev. B **56**, R505 (1997).
[5] K. Ishida *et al.*, Nature (London) **396**, 658 (1998); Phys. Rev. B **63**, 060507(R) (2001).
[6] G. M. Luke *et al.*, Nature (London) **394**, 558 (1998).
[7] T. M. Riseman *et al.*, Nature (London) **396**, 242 (1998); P. G. Kealey *et al.*, Phys. Rev. Lett. **84**, 6094 (2000).
[8] T. M. Rice and M. Sigrist, J. Phys. Cond. Mat. **7**, L643 (1995); M. Sigrist *et al.*, Physica C **317-318**, 134 (1999).
[9] S. NishiZaki, Y. Maeno, and Z. Mao, J. Phys. Soc. Jpn. **69**, 572 (2000).
[10] K. Ishida *et al.*, Phys. Rev. Lett. **84**, 5387 (2000).
[11] I. Bonalde *et al.*, Phys. Rev. Lett. **85**, 4775 (2000).
[12] M. A. Tanatar *et al.*, Physica C **341-348**, 1841 (2000); Phys. Rev. B **63**, 064505 (2001).
[13] H. Matsui *et al.*, Phys. Rev. B **63**, 060505(R) (2001).
[14] C. Lupien *et al.*, Phys. Rev. Lett. **86**, 5986 (2001).
[15] Vertical and horizontal lines of nodes were discussed for cuprates by R. J. Radtke, A. I. Liechtenstein, V. M. Yakovenko, and S. Das Sarma, Phys. Rev. B **53**, 5137 (1996).
[16] K. Miyake and O. Narikiyo, Phys. Rev. Lett. **83**, 1423 (1999).
[17] Y. Hasegawa, K. Machida, and M. Ozaki, J. Phys. Soc. Jpn. **69**, 336 (2000).
[18] M. J. Graf and A. V. Balatsky, Phys. Rev. B **62**, 9697 (2000).
[19] H. Won and K. Maki, Europhys. Lett. **52**, 427 (2000).
[20] D. F. Agterberg, T. M. Rice, and M. Sigrist, Phys. Rev. Lett. **78**, 3374 (1997).
[21] M. E. Zhitomirsky and T. M. Rice, Phys. Rev. Lett. **87**, 057001 (2001).
[22] M. A. Tanatar *et al.*, Phys. Rev. Lett. **86**, 2649 (2001); K. Izawa *et al.*, *ibid.* **86**, 2653 (2001).
[23] T. Dahm, H. Won, and K. Maki, cond-mat/0006301.
[24] S. Kashiwaya *et al.*, Phys. Rev. B **51**, 1350 (1995); M. Covington *et al.*, Phys. Rev. Lett. **79**, 277 (1997); J. Y. T. Wei *et al.*, *ibid.* **81**, 2542 (1998).
[25] C.-R. Hu, Phys. Rev. Lett. **72**, 1526 (1994); J. Yang and C.-R. Hu, Phys. Rev. B **50**, 16766 (1994).
[26] M. Yamashiro, Y. Tanaka and S. Kashiwaya, Phys. Rev. B **56**, 7847 (1997); M. Yamashiro, Y. Tanaka, Y. Tanuma, and S. Kashiwaya, J. Phys. Soc. Jpn. **67**, 3224 (1998); N. Yoshida, Y. Tanaka, J. Inoue, and S. Kashiwaya, *ibid.* **68**, 1071 (1999); M. Yamashiro, Y. Tanaka, N. Yoshida, and S. Kashiwaya, *ibid.* **68**, 2019 (1999).
[27] C. Honerkamp and M. Sigrist, J. Low T. Phys. **111**, 895 (1998).
[28] F. Laube *et al.*, Phys. Rev. Lett. **84**, 1595 (2000).
[29] Z. Q. Mao *et al.*, Phys. Rev. Lett. **87**, 037003 (2001).
[30] G. E. Blonder, M. Tinkham, and T. M. Klapwijk, Phys. Rev. B **25**, 4515 (1982).
[31] Y. Tanaka and S. Kashiwaya, Phys. Rev. Lett. **74**, 3451 (1995).
[32] K. Sengupta *et al.*, Phys. Rev. B **63**, 144531 (2001).
[33] M. Sigrist and H. Monien, cond-mat/0102464.